



Use of models and observations to assess trends in the 1950–2005 water balance and climate of Upper Klamath Lake, Oregon

S. W. Hostetler¹

Received 18 July 2008; revised 6 August 2009; accepted 26 August 2009; published 12 December 2009.

[1] A 1-dimensional surface energy balance model is applied to produce continuous simulations of daily lake evaporation of Upper Klamath Lake, Oregon (UKL) for the period 1950–2005. The model is implemented using observed data from land-based sites and rafts collected during 2005–2006. Progressively longer, temporally overlapping simulations are produced using observed forcing data sets from sites near UKL. Simulation of the entire 56 years is accomplished using forcing data derived from weather station data and a 1949–2007 regional climate simulation over western North America. Simulated mean annual evaporation for 1950–2005 is 1073 mm. The simulated evaporation estimates are an improvement over existing May–September pan-derived estimates because the latter are not representative of annual evaporation rates and do not span the multidecadal period of interest over which climate-driven interannual (and longer) variability is evident. Evaporation and the other components of the water balance display statistically significant trends over the past 56 years that are associated with changes in meteorological forcing over the lake and the radiative and moisture balances at higher elevations of the catchment. Trends in the basin are consistent with and imbedded in regional and hemispheric climate trends that have occurred over the last century.

Citation: Hostetler, S. W. (2009), Use of models and observations to assess trends in the 1950–2005 water balance and climate of Upper Klamath Lake, Oregon, *Water Resour. Res.*, 45, W12409, doi:10.1029/2008WR007295.

1. Introduction

[2] Measurements at the Klamath Falls Experimental Station and NRCS SNOTEL sites indicate that precipitation over the Upper Klamath Lake basin (UKL) was about 50% of normal during 2000–2001. The ensuing drought-related water shortage led to serious conflicts over allocating water for irrigators and maintaining water allocations mandated under the Endangered Species Act (ESA) to protect habitat for suckers in Upper Klamath Lake and Coho salmon in the lower Klamath basin. The joint involvement in the basin of irrigators, Federal, state, county, and local agencies and private utilities led to public hearings, assessments of the water balance and biologically based water needs [e.g., Braunworth *et al.*, 2001; Perry *et al.*, 2004], and, ultimately, to a large effort by the National Research Council aimed at evaluating water management and ESA requirements in the basin [National Research Council, 2008]. Water related research in the basin is ongoing [e.g., Wood *et al.*, 2006; Gannett *et al.*, 2007; Morace, 2007].

[3] UKL lies in a semiarid climatic zone; the primary source of water for the lake is derived from snowpack that accumulates in the mountainous areas of the catchment and water loss occurs predominately through evaporation and

river discharge. Interannual and longer-term climate variability play a key role in determining both winter accumulation of mountain snowpack and summer water loss and demand during the season of peak irrigation diversion and minimum stream flow. Some of the components of the lake water balance are well known (e.g., Williamson River inflow and Klamath River outflow into the Link River and A-Canal) while others are less certain (evaporation, ungauged input from streams, net groundwater flow and irrigation return flow), particularly over long time periods.

[4] Estimates of evaporation from UKL derived from evaporation pan measurements range from 720 mm a⁻¹ to 1116 mm a⁻¹ [Perry *et al.*, 2004] (see also Bureau of Reclamation, AgriMet—The Pacific Northwest cooperative agricultural weather network, <http://www.usbr.gov/pn/AgriMet/> and Comparative climate western states, pan evaporation, available at <http://www.ocs.orst.edu/>). An evaporation rate of 1000 mm a⁻¹ is roughly double the long-term average of over-lake precipitation, is about equal to the flow of the Wood River, the second largest tributary to the lake, and is roughly one third of the flow of the Williamson River which is the largest river flowing into the lake. Given the magnitude of evaporation in the lake hydrologic budget, it is useful to quantify climatically driven evaporation rates (1) to help achieve better closure of the water balance, (2) to reduce uncertainties regarding the volume of inflow from ungauged streams and groundwater, (3) to allow near real-time computations of evaporation rates and (4) to investigate the nature of long-term variability and change in the forcing climatology.

¹U.S. Geological Survey, Department of Geosciences, Oregon State University, Corvallis, Oregon, USA.

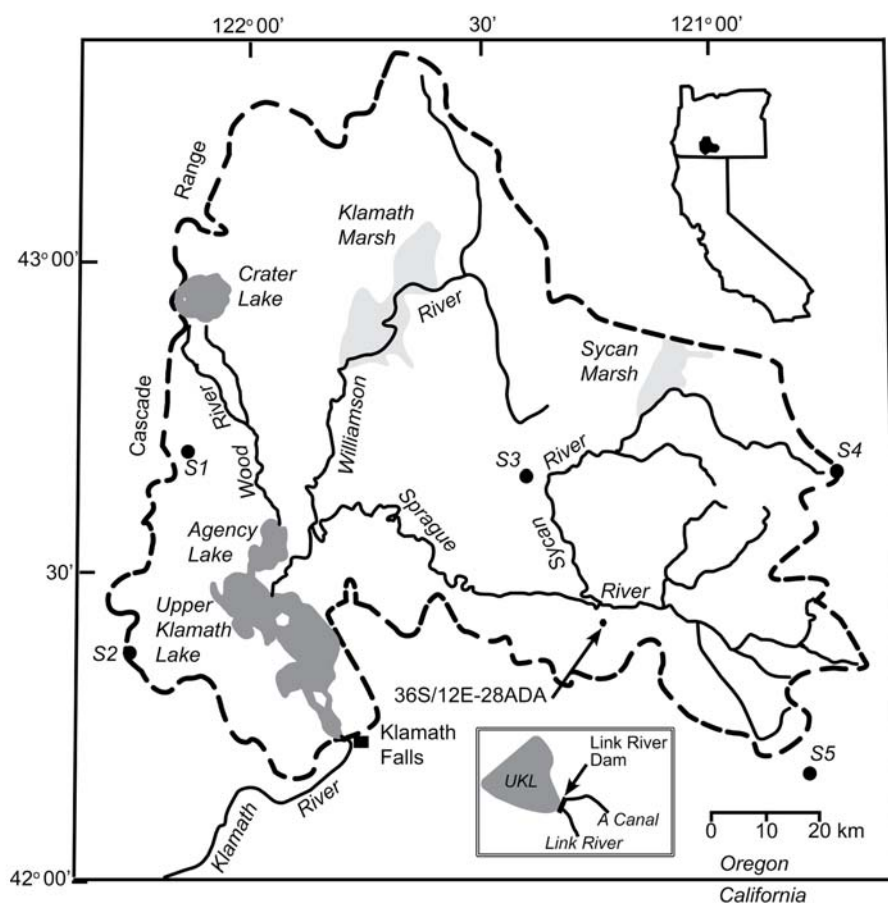


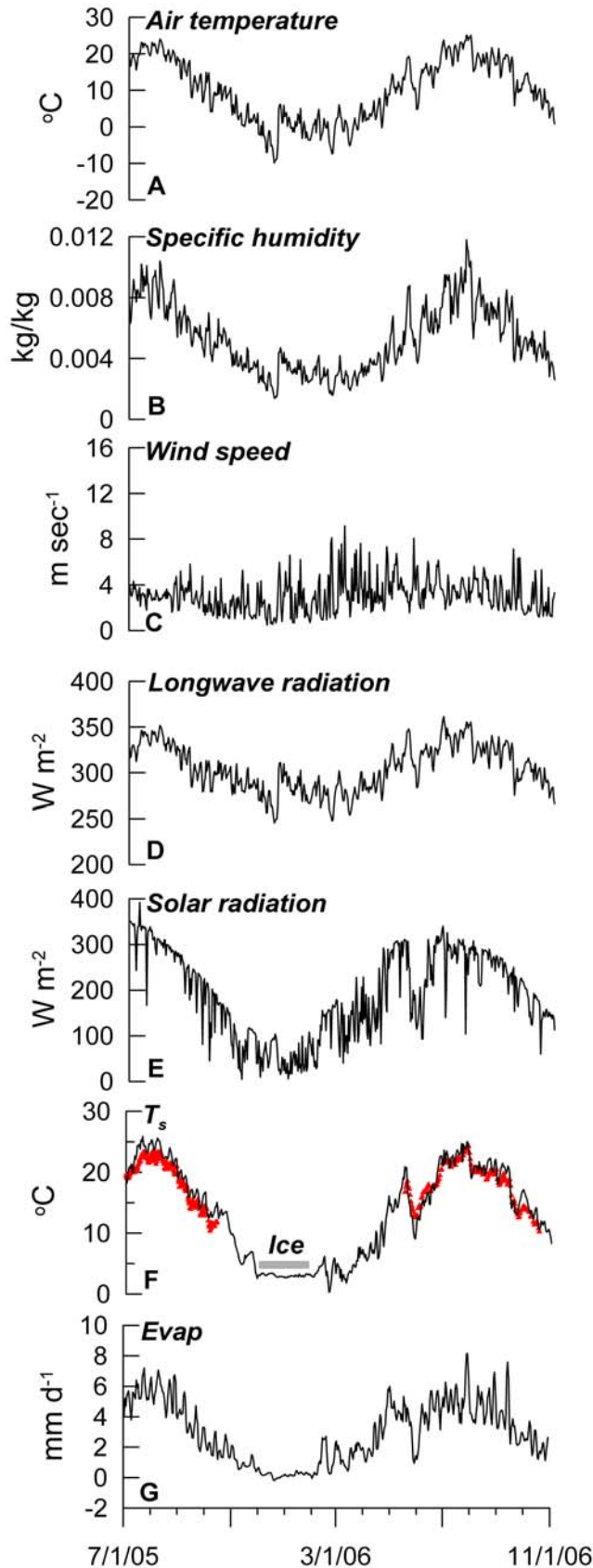
Figure 1. Location map of Upper Klamath Lake and basin. The approximate location of the USGS well 422508121161501 36S 12E-28ADA discussed in the text is shown. The inset (not to map scale) illustrates outflow distribution below Link River Dam into the Link River (which flows into the Klamath River) and A-Canal which is used to convey irrigation water. The approximate locations of NRCS SNOTEL sites discussed in the text are indicated by S1, Seven Mile Marsh; S2, Billie Creek Divide; S3, Taylor Butte; S4, Summer Rim; and S5, Quartz Mountain.

[5] This paper presents an analysis of the water balance of UKL over the past 56 years using a combination of observed climate and streamflow data and climate fields simulated with a regional climate model. A 1-D lake model is applied to simulate lake evaporation. The lake model is calibrated and validated using 2005–2006 meteorological data collected at four land-based sites and two rafts on the lake. Longer, temporally overlapping simulations are conducted using archived data sets derived from the U.S. Bureau of Reclamation AgriMet station and the regional climate model. The analysis identifies multidecadal climate change over UKL and the UKL basin, assesses the sensitivity of the UKL water balance to those changes and places climate trends in the context of changes that have occurred over western North America. The magnitude of climate-driven change in the water balance suggests that the changes need to be integrated into decisions regarding allocation of water in the basin.

2. Basin Description

[6] UKL is a large, shallow water body (232 km², mean depth 2.8 m) with a drainage basin that covers 9,415 km²

[Risley and Laenen, 1998; Wood et al., 2006; Gannett et al., 2007]. The lake is located in the high desert of south-central Oregon, east of the Cascade Range (Figure 1). The climate of the basin is continental, but winters are moderated by Pacific storms that move over the Cascades. Annual precipitation ranges from over 1500 mm in the higher elevations of the Cascades to around 300 mm at lower elevations that lie in the rain shadow of the Cascades. The mean annual air temperature near the lake is ~8°C. Surface water inputs to the lake are dominated by the Williamson River which is comprised of the upper Williamson, Sycan and Sprague Rivers. The tributaries receive runoff directly from the mountainous areas of their catchments and from large marsh areas on the valley floor. The Wood River, which originates in the Cascades on the south side of the Crater Lake caldera, is the second largest source of water for the lake. Other water sources include ungauged streams from the west and groundwater; the magnitudes of these sources are estimated indirectly [Miller and Tash, 1967; Hubbard, 1970; Gannett et al., 2001; Perry et al., 2004; Gannett et al., 2007]. Outflow from the lake is regulated by the dam at the south



end of the lake, and passes into the Link River and the A-Canal, and ultimately into the Klamath River.

3. Lake Model Description and Validation

[7] The lake model used here is a one-dimensional model that simulates lake temperature, heat fluxes, evaporation and lake ice in response to meteorological forcing [Hostetler and Bartlein, 1990]. Heat is transported vertically in the water column by eddy diffusion and convective mixing. The model is written as

$$\frac{\partial T}{\partial t} = \frac{\partial}{\partial z} \left\{ [k_m + K(z, t)] \frac{\partial T}{\partial z} \right\} + \frac{\partial \Phi}{\partial z} \quad (1)$$

where T is water temperature, t time, z depth, k_m molecular diffusivity, K eddy diffusion, and Φ is a heat source term representing absorption of penetrating solar radiation. The surface energy balance is incorporated into the surface boundary condition as

$$\frac{\partial T}{\partial z} [k_m + K(z, t)] = \frac{1}{C} [(1 - \alpha)\phi_s + \phi_i - \phi_o - q_l - q_h] \quad (2)$$

where C is thermal heat capacity, α is the shortwave albedo of the water surface, ϕ_s downward solar radiation, ϕ_i downward longwave radiation, ϕ_o longwave radiation from the surface, q_l latent heat flux and q_h sensible heat flux.

[8] Latent heat flux is computed in the model

$$q_l = C_D U_2 \rho \Delta q L_e \quad (3)$$

where C_D is the drag coefficient which is a nonlinear function of the bulk Richardson stability number, U_2 is the 2 m wind speed, ρ is the density of the surface air (0.997), Δq is the vapor pressure gradient between the water surface and the overlying atmosphere, and L_e is the latent heat of vaporization of water.

[9] Sensible heat flux is computed using a similar bulk transfer equation

$$q_h = C_D U_2 \rho c_p \Delta T \quad (4)$$

where c_p is the heat capacity of air and ΔT is the air-water temperature difference.

[10] Wind-driven eddy diffusion is computed using the closure method of Henderson-Sellers [1985]. Convective mixing is density driven, and is used to smooth temperature profiles primarily during cooling periods in autumn. The model also includes a submodel that is used to simulate lake ice. Further details and relevant applications of the model are given in Hostetler and Bartlein [1990], Hostetler and

Figure 2. Observed 2005–2006 daily meteorological inputs for the lake model: (a) 2-m air temperatures, (b) specific humidity, (c) wind speed, (d) atmospheric long wave radiation, and (e) incident shortwave radiation. Lake model simulations of (f) 1 m water temperature and lake ice and (g) evaporation. Simulated 1 m lake temperature is compared with observed values at two raft locations (red pluses).

Table 1. Lake Model Inputs Averaged Over the Indicated Calendar Years^a

	TS2 (°C)	Q (kg kg ⁻¹)	U (m s ⁻¹)	SW (W m ⁻²)	LW (W m ⁻²)	Precipitation (mm)
			2005–2006			
Obs	8.1	0.0049	3.1	175.0	300.1	
KFLO	8.2 ± 8.5	0.0043 ± 0.002	2.3 ± 1.4	181.1 ± 101.7	294.5 ± 35.9	294.0
RegCMB	8.2 ± 8.5	0.0047 ± 0.002	4.1 ± 3.6	187.5 ± 99.1	294.5 ± 35.9	1025
			2002–2006			
KFLO	8.5 ± 8.1	0.0043 ± 0.002	2.4 ± 1.3	181.7 ± 97.9	295.5 ± 34.1	308.0
RegCMB	8.5 ± 8.1	0.0046 ± 0.002	4.1 ± 3.4	185.4 ± 95.5	295.5 ± 34.1	883.0
			1950–2005			
RegCMB	8.9 ± 8.3	0.0048 ± 0.002	5.6 ± 4.5	186.3 ± 95.5	297.5 ± 35.2	950

^aObs, from the meteorological stations on UKL; KFLO, from the Klamath Falls AgriMet station; RegCMB, from the regional climate model. TS2, 2 m air temperature; Q, specific humidity; U, wind speed; SW, shortwave radiation; LW, atmospheric longwave radiation.

Giorgi [1993, 1995], Small *et al.* [1999], and Hostetler and Small [1999].

[11] For the lake model simulations, the lakes (Klamath and Agency) were represented by a digital elevation model of 27,313 grid points with 100 m spacing and water depths ranging from 2 to 15 m. The 1-D model was run on a daily time step at each water grid point. The observed data set used to drive the lake model (Figure 2) includes observations at four land and two raft-based sites generated as part of an ongoing water quality study being conducted by the USGS at UKL [Wood *et al.*, 2006]. Data are recorded as 15 min averages at the sites. The number and types of sensors varies among the sites, and there were periods of lost data at each site; however, with two exceptions each input variable were available from at least one site at all times during the simulation period. Daily average data for the lake model was derived by averaging the 15 min observations interpolated to each water grid point using a distance-weighted function that included all available station data. A short gap of about a week in the recorded data for solar radiation during the winter of 2006 was filled in with data collected by the University of Oregon Solar Monitoring Laboratory at the Klamath Falls site (available at <http://solardat.uoregon.edu/index.html>).

[12] Prior to installation of a precision longwave radiometer in the fall of 2005, downward atmospheric radiation is computed as

$$\phi_l = 0.85(0.97\sigma T^4) \quad (5)$$

where σ is the Stefan-Boltzman constant and T is air temperature. The factor of 0.85 scales the computed radiation values such that the mean of the computed values is the same as that of the measured values. More complex methods for computing longwave radiation that account for atmospheric humidity and cloud cover exist [e.g., Anderson, 1954; Brutsaert, 1982; Henderson-Sellers, 1986], but equation (5) requires less data (more complex methods require daily cloud cover which is not available at UKL), uses a constant scaling factor of 0.85, and is adequate for computing longwave radiation for the longer multiyear simulations discussed, for which there are no measurements of longwave radiation. The input data set is summarized in Table 1.

[13] The lake model simulates the seasonal cycle and shorter-term variability of lake surface temperature associated with synoptic-scale circulation such as the passage of fronts (Figure 2); the root-mean-square error (RMSE) between simulated and observed water temperatures is 1.8°C.

For comparison, the standard deviation of observed raft temperatures is 3.8°C over the period July through mid-October, 2005 and May through October, 2006. Periods of stratification (not shown) were simulated during the summer at the deeper lake grid points, but stratification persisted only for a few days before being broken down by wind-driven and convective mixing. The shallower lake grid points remained well mixed and isothermal. The largest discrepancies between the simulated and measured lake temperatures likely indicate the lack of 3-D circulation in the lake model [Wood *et al.*, 2008; T. Wood, personal communication, 2008]. Persistent lake ice was simulated during the winter over the shallowest water grid points and periods of full-lake ice cover were simulated during December through February. Simulated lake evaporation, which is tightly coupled to lake surface temperature through the energy balance, mirrors the seasonal cycle of climate and features of lake temperature (Figure 2). Periods of condensation are evident in the late fall and early winter before the lake freezes. The average simulated surface temperature for the 2005–2006 period is 11.0°C; annual evaporation is 994 mm, and irrigation season evaporation (May–September) is 707 mm (Table 2).

Table 2. Simulated and Derived Values of Lake Surface Temperature and Evaporation^a

	T _s (°C)	RMSE (°C)	Evaporation (mm d ⁻¹)	Evaporation (mm a ⁻¹)
			2005–2006	
Obs	11.0 ± 7.6	1.78	2.7 ± 2.2	994
KFLO	11.3 ± 7.4	1.60	2.9 ± 2.8	1048
RegCMB	11.0 ± 8.0	2.06	2.8 ± 2.8	1009
Pan derived	–	–	2.8	776 ^b (1015) ^c
			2002–2006	
KFLO	11.0 ± 7.0	1.65	2.9 ± 2.6	1050
RegCMB	10.6 ± 7.2	2.01	2.9 ± 2.8	1052
Pan derived	–	–	2.8	1038
			1950–2005	
RegCMB	10.9 ± 7.1	–	2.9 ± 3.0	1073
Pan derived	–	–	–	776 ^b (1015) ^c

^aObs, simulated using the observed meteorological data from the lake; KFLO, simulated using the meteorological data from the KFLO AgriMet station; RegCMB, simulated using the blended RegCM output and observed data; Pan derived, evaporation estimates derived from NOAA observations. T_s, surface temperature; RMSE, root-mean-square error between simulated and observed T_s; Evaporation, lake evaporation averaged over the indicated calendar years.

^bUsing a pan coefficient of 0.7 applied to open-water (May–September) pan measurements.

^cUsing a pan coefficient of 0.7 applied to synthesized full-year evaporation pan measurements.

[14] Daily pan measurements (E_p) for the NOAA weather station (KFalls_2_ssw) obtained from NOAA station archives were used to evaluate simulated evaporation. These records span the ice-free months (generally May or June through September or October) of 1978–1987 and 1997–2003. The long-term average May–September evaporation derived from the warm season pan measurements is 776 mm, a value $\sim 9\%$ greater than the simulated May–September value of 707 mm. Because roughly 30% of the annual simulated evaporation occurs during the spring and fall, full-year pan estimates were derived using the 1999–2006 seasonal cycle of evapotranspiration (ET) computed for the KFLO AgriMet station (<http://www.usbr.gov/pn/AgriMet/>) to distribute the annual pan values into a percentage by month.

[15] Evapotranspiration is computed by the Bureau of Reclamation from well watered alfalfa plots using the Penman-Kimberly method [Allen *et al.*, 2005]. The computed values are thus adequate estimates of potential evapotranspiration (PET) [e.g., Kahler and Brutsaert, 2006]. May through September PET is $\sim 73\%$ of the annual total, confirming that 27% of annual PET (and thus pan evaporation) occurs outside the usual observation period for E_p . To estimate the annual rate of E_p , the available monthly measurements and the PET-based distribution were used to fill in the missing months (there is no lag in the timing of the seasonal cycles in the pan and PET measurements), which yielded an average lake evaporation rate of $1015 \pm 88 \text{ mm a}^{-1}$ based on a pan transfer coefficient of 0.7. The transfer coefficient is a nominal value and there are additional uncertainties associated with specifying a value [Masoner *et al.*, 2008]. For an average surface area of UKL, 27% of the annual evaporation not accounted for by pan measurements amounts to $\sim 8 \times 10^9 \text{ m}^3$ (18,105 acre feet) of water.

4. Lake Model Implementation

[16] The goal of the lake modeling is to produce a long-term simulation of climate-driven evaporation optimized by minimizing the difference between simulated and observed lake surface temperature and joint analysis of observed and derived lake evaporation. Ideally, an observed input data set similar to the 2005–2006 data on and adjacent to the lake would be available, but no such data set exists. To assess the reliability of applying the lake model to simulate 1950–2006 evaporation, three progressively longer and temporally overlapping data sets were used to derive daily inputs for the lake model: 1999–2006 data collected at the USBOR KFLO AgriMet site, data collected at the KFalls_2_ssw NOAA weather station, and data for 1950–2006 from a regional climate model simulation over western North America [Hostetler *et al.*, 2006].

[17] The regional climate model, RegCM, couples the RegCM2 atmospheric model of Giorgi *et al.* [1993] to a full physics, six layer, land surface model, LSX [Thompson and Pollard, 1995]. LSX simulates the surface energy and water balances (e.g., evaporation, runoff, soil temperature and moisture, snow and ice) over soil, water, vegetation and permanent ice in response to exchanges of energy, mass and momentum between the surface and the boundary layer. A key advantage of climate models is that they simulate a large number of internally consistent, time-varying atmo-

spheric and surface variables over areas where observations are incomplete, sparse, or nonexistent. A good example is solar radiation at the surface which is mediated by clouds and atmospheric composition (e.g., aerosols, optical air mass).

[18] The data set from the regional climate model was derived from a 56 year simulation of western North America which was run with a horizontal grid spacing of 45 km using time varying (6 h) lateral boundary conditions and sea surface temperatures derived from the NCEP-NCAR reanalysis data [Kistler *et al.*, 2001]. Input data sets for the lake model were obtained by bilinear interpolation of the four RegCM grid points closest to UKL. Three of the four grid cells are located in the (smoothed) model representation of the Cascades (e.g., at Crater Lake) so air temperature, and thus long wave radiation were elevation corrected to UKL using a nominal atmospheric lapse rate of $-6.5^\circ\text{C km}^{-1}$. Further details of RegCM and the simulation are given by Hostetler *et al.* [2006].

[19] For the 1950–2006 period, the average RegCM air temperature for UKL is $7.1 \pm 10^\circ\text{C}$ compared to the observed average at the KFalls_2_ssw NOAA weather station which is $8.9 \pm 8.3^\circ\text{C}$, indicating a cold bias in the RegCM data. The cold bias is attributed to the snowpack that accumulates on the higher elevation RegCM grid points: until the snow melts in the spring, air temperatures remain cool, and shortwave albedo is relatively high compared to open ground. After the snow melts, the RegCM air temperatures are in good agreement with observations at UKL. To minimize the late spring biases in the RegCM data used for the lake model, a blended data set (hereafter denoted RegCMB) was derived by substituting observed air temperature data from the KFalls_2_ssw NOAA weather station for the RegCM air temperatures. To account for first order temperature dependencies on air temperature, in the blended data set, humidity from the RegCM was adjusted to reflect differences in the NOAA air temperatures and longwave radiation was recomputed using the NOAA temperatures.

[20] Over the 2005–2006 validation period (Figure 2), the forcing data sets are similar both in the patterns of their time series and the related statistics (Figure 3 and Table 1). The largest departures from the daily time series for all variables are exhibited in the data simulated by the RegCM. Brief peaks in simulated wind speeds during winter are associated with storms in the Cascades that are apparent, but attenuated in the AgriMet data. Similar periods of low wind speeds are simulated throughout mid-2006. The forcing data sets yield simulated lake temperatures that are in good agreement with measurements at the rafts (Figure 3 and Table 2). Again, the seasonal cycle, interannual variability resulting from synoptic-scale weather patterns (e.g., June, 2006), are reproduced in all simulations. Evaporation rates simulated with the various forcing data sets also are comparable both in structure (Figure 3 and Table 2) and in their statistics.

[21] Comparisons of longer lake simulations with measured lake temperature data for the period 2002–2006 (Figure 4a) include a period for which pan evaporation data are available (Figure 4b). Input data sets for the lake model derived from the RegCMB and KFLO AgriMet station have a common period of overlap beginning in 1999. Simulated

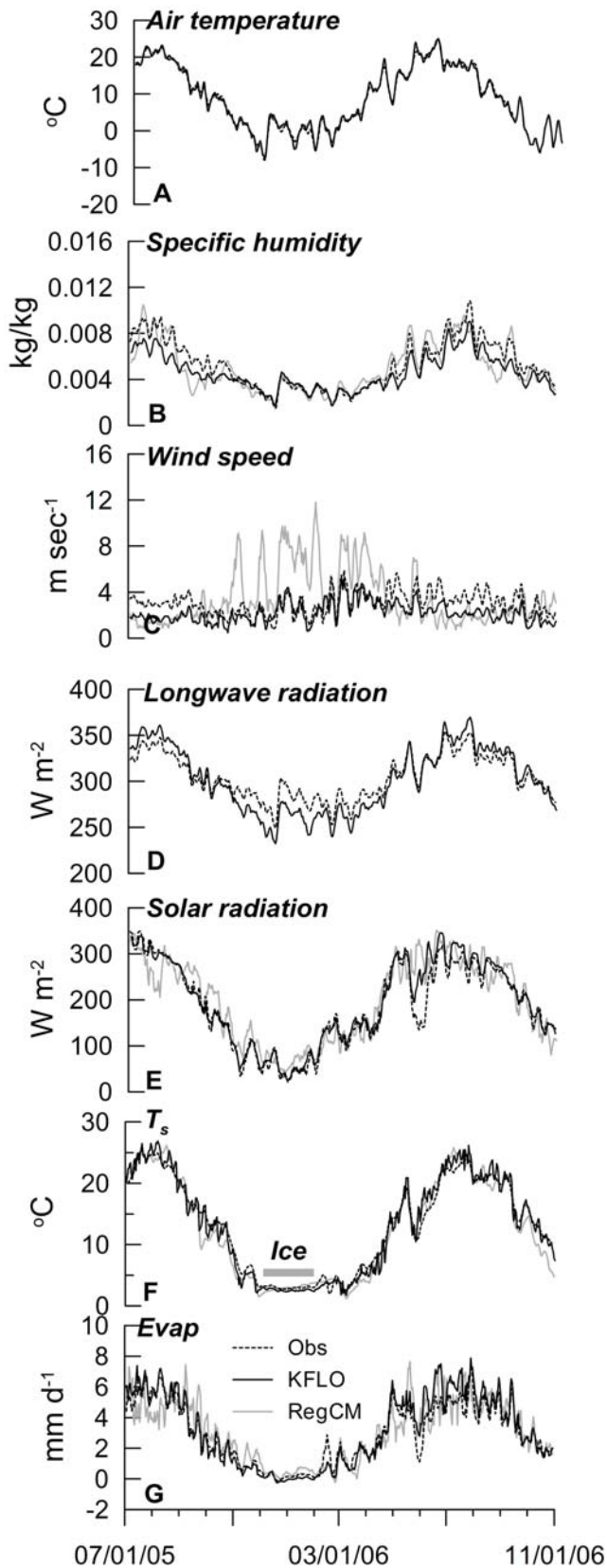


Figure 3. As in Figure 2 with time series added for Klamath Lake, OR AgriMet station (KFLO), and the RegCMB.

surface temperatures averaged over the lake compare very well with the aggregated observed data (Figure 4 and Table 2). The RegCMB data produces more variability than the AgriMet data sets, and short-term maximum summer temperatures are too warm in 2005 and 2006 as a result of forcing and the 1-D limitations of the model, but the multiyear seasonal cycle and interannual variability are well simulated.

[22] Additional estimates of lake evaporation were derived by converting the monthly PET to monthly E_p and then scaling the E_p values to lake values. Scaling coefficients to convert PET to E_p vary depending on wind fetch, wind speed, humidity, and climatic setting [Snyder *et al.*, 2005]. Based on experimental results for sites in California, a reasonable value for the scaling coefficient for the KFLO site is 1.27 [Snyder *et al.*, 2005] so that $E_p = 1.27PET$ and $E = 0.7E_p$. The resulting 2002–2006 average value of $1148 \pm 47 \text{ mm a}^{-1}$ is $\sim 13\%$ greater than the pan-derived value of 1015 mm a^{-1} discussed above and is 9% greater than the simulated value of $\sim 1052 \text{ mm a}^{-1}$.

[23] Although pan and PET data are often used to derive estimates of lake evaporation, there are several drawbacks to their use, including a lack of a full seasonal cycle of E_p values in colder climates such as that of UKL, variability of pan coefficients related to physical location and climate [e.g., Brutsaert, 1982] and potentially large differences in the energy balances associated with lake heat storage [e.g., Dutton and Bryson, 1962]. These uncertainties potentially diminish the usefulness of such estimates, particularly with respect to interannual climatic forcing. The overall agreement of model simulated evaporation with the values

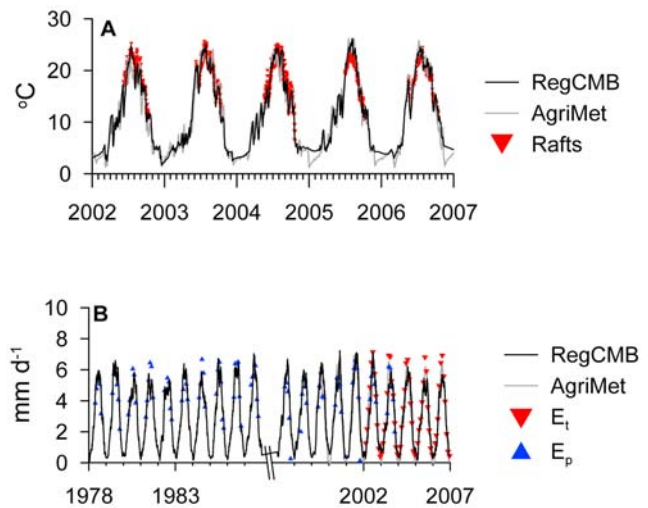


Figure 4. (a) Time series of daily 1 m water temperature for the period 2002–2006 simulated by the lake model using the RegCMB and KFLO AgriMet data sets as input compared with available lake temperature data (red triangles) collected at raft sites by the USGS. (b) Time series of monthly evaporation for the periods 1978–1988 and 1997–2006 simulated by the lake model using the RegCMB and KFLO AgriMet data sets as input compared with derived, full-year pan evaporation estimates (red triangles) for the KFalls_2_ssw NOAA weather station and with scaled potential evapotranspiration from the AgriMet Station (blue triangles).

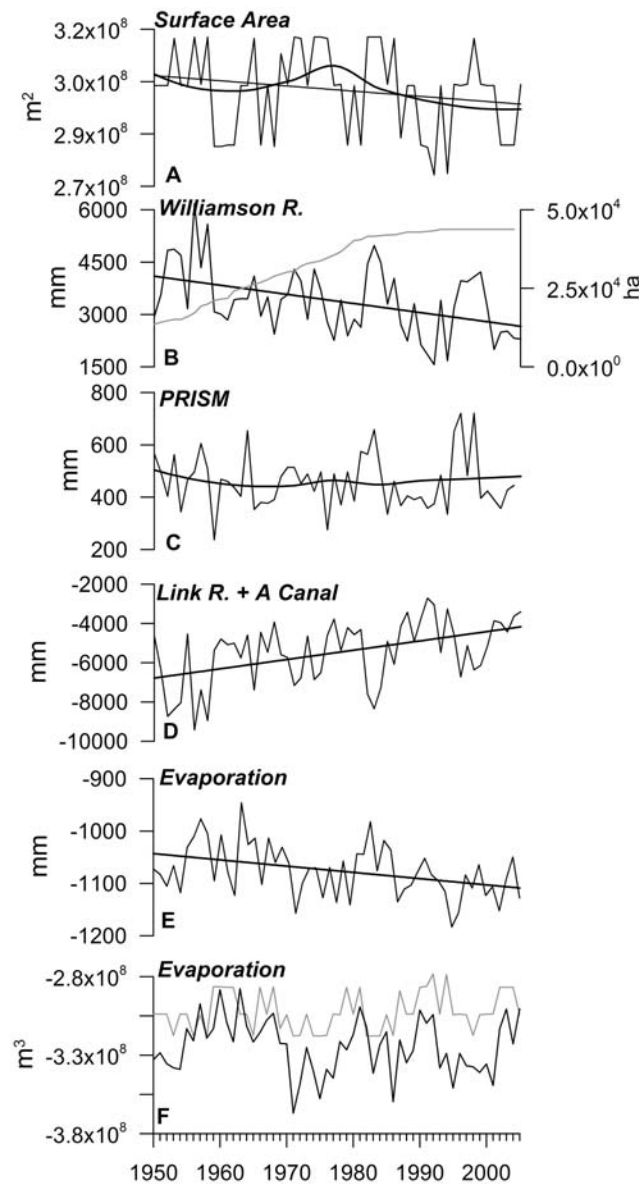


Figure 5. Time series of annual values of lake surface area and the components of the 1950–2005 water balance of UKL. Significant trends (at the $p < 0.01$ level and greater) are indicated by the linear fits and LOWESS curves are fit to time series lacking significant trend. Water inputs are plotted as positive values and water outputs are plotted as negative values. (a) Annual average surface area, (b) Williamson River (thick line) and irrigated hectares in the Sprague and Williamson basins, (c) precipitation at UKL from the PRISM data set [Daly et al., 1994], (d) combined discharge from UKL in the Link River and A-Canal, (e) Simulated evaporation from the lake model, and (f) water volume computed for simulated evaporation (thick line) and estimated from using a fixed pan value of 1057 mm a^{-1} . Irrigation data from Risley and Laenen [1998] and the Oregon Water Resources Department Water Right database (<http://www.wrd.state.or.us/OWRD/WR/wris.shtml>).

derived for ET and pan evaporation, and the consistency of the simulated values across the range of observed and modeled input data sets lend support to application of the

lake model to produce multidecadal evaporation data for analyses of the long-term water balance of UKL.

5. The 1950–2005 UKL Water Balance

[24] Annual values of the UKL water balance were calculated using measured inflow and discharge data, along with simulated evaporation and over-lake precipitation rates obtained from the gridded PRISM data (Figure 5 and Table 3). Calendar year records for the gauging stations on the Wood River (USGS gauges 11504100 and 115040000) are complete only for the periods 1923–1935 and 1965–1966, so a discharge record was constructed using linear regression with observed records of the Williamson River. There are uncertainties associated with Wood River records because the gauges are not located at the outlet to the lake and the warm season discharge is affected by upstream irrigation withdrawals and return flows.

[25] Wetlands and marsh bordering UKL cover $\sim 70 \text{ km}^2$ [Snyder and Morace, 1997; Bradbury et al., 2004] and evapotranspiration and precipitation over these areas are additional paths of water loss and gain for UKL. Open-water evaporation is generally greater than PET of wetlands. Actual ET is somewhat less than PET due to seasonal changes in vegetation which affects transpiration rates and fractional vegetative cover. Various methods have been used to compute ET from wetlands using detailed, high resolution meteorological data [e.g., Bidlake, 2002; Drexler et al., 2004], but all require numerical parameters to be specified or fitted, and computed ET values are quite sensitive to the selected values. In addition, adequate field data for validating the ET computations do not exist at UKL. For this analysis, an evapotranspiration rate of 85% of the simulated open water evaporation rate for UKL [Risley and Gannett, 2006] was specified, which yielded a mean annual wetland

Table 3. The 1950–2005 Annual Average Water Balance Components of UKL Expressed in Volume and Depth Over the Mean Lake Surface Area^a

	Volume ^b ($\text{m}^3 \times 10^9$)	Percent of Total Water Sources and Losses
Sources		
Williamson River	1.01 (3381)	50.25 (49)
Wood River ^c	0.28 (947)	13.93 (16)
Over-lake precipitation ^d	0.14 (460)	6.97 (7)
Groundwater, springs and seeps	0.33 ^e (1105)	16.42 (14) ^f
Other ^g	0.25 (836)	12.44 (14)
Total Inputs	2.01 (6729)	100
Losses		
Link plus A-Canal	1.64 (5472)	80.79 (78)
Open-water evaporation	0.32 (1075)	15.76 (20)
Wetland evapotranspiration	0.07 (235)	3.45 (–)
Total Losses	2.03 (6782)	100
Change in Storage	0.00	–
Residual	–0.02 (53)	

^aParenthetical values are those of Hubbard [1970].

^bVolume is given in equivalent depth mm.

^cReconstructed by regression.

^dPRISM data for Klamath Lake grid point.

^eFrom Perry et al. [2004].

^fHubbard [1970] water balance residual.

^gOther is irrigation returns and ungauged streams.

ET of 912 mm ($0.072 \times 10^9 \text{ m}^3$ over the mean lake area). Losses through ET thus account for only about 3.5% of total loss in the lake water balance. At a maximum rate of PET equal to open water evaporation, ET losses would be <4% of the total water loss.

[26] The water balance of UKL is dominated by inputs from the Williamson and Wood Rivers and outflow into the Link River and A-Canal which amount to ~64% and ~81% of the water inputs and outputs, respectively (Figures 5b and 5d and Table 3). *Perry et al.* [2004] calculated groundwater flow (springs and seeps) into the lake to be about $0.33 \times 10^9 \text{ m}^3$ (271,000 acre feet) based on a detailed analysis of gauged water inflows and outflows and lake stage. Precipitation over the lake is ~7% of the total water input (Figure 5c). *Hubbard* [1970] estimated that canals, ungauged streams, and agricultural returns contribute 14% of the total inflows to UKL. Both the estimates of *Perry et al.* [2004] and *Hubbard* [1970] were used in the water balance computations in Table 3.

[27] Open-water evaporation amounts to ~16% of the total water losses (Figure 5e, and Table 3) from UKL. Substantial climate-driven interannual variability is evident in the evaporation rates (Figure 5e). Fixed lake evaporation derived from pan values underestimates the climatically determined variability of simulated evaporation by an average of ~7%; however, differences between annual simulated and pan evaporation rates range from -6% in 1962 to 15% in 1994, with a period of particularly large departures evident in the 1970s and 1990s. The volume of water associated with the 1994 departure is $0.05 \times 10^9 \text{ m}^3$ (42,335 acre feet).

[28] Based on the measured, simulated, and estimated values, the 1950–2005 average water balance residual is $-0.02 \times 10^9 \text{ m}^3$ (16,050 acre feet) (Table 3), indicating that the budget is essentially balanced, assuming that about 12% of water inputs to the lake are accounted for in ungauged streams and irrigation returns. The balance of inputs and outputs is only slightly modulated by operation of the Link River Dam because change in UKL storage is limited to a very small range (mean annual lake elevation varies by only ± 21 cm, Figure 5a). It is difficult to get a precise estimate of uncertainty in the measured water balance components, but it is likely that the uncertainty lies in the range of ± 10 –15%; the range of uncertainty in the estimates of groundwater and other inputs is at least as large.

6. Multidecadal Trends and Characteristics

[29] The water balance and related climate time series were analyzed for trends. Some of the annual time series are autocorrelated (at lag 1). Autocorrelation is problematic because the *t* test used for hypothesis testing of the slope assumes serial independence of the residuals from the trend line and lack of independence can lead to more rejections of the null hypothesis (no trend) than are warranted (i.e., falsely indicating a trend) at the selected level of significance [*von Storch and Zwiers*, 1999; *Yue et al.*, 2002]. Partial autocorrelation and autocorrelation functions for each variable were computed and plotted, and the plots were used to assess the presence of serial correlation [*Box and Jenkins*, 1976; *von Storch and Zwiers*, 1999]. When autocorrelation was present, the approach of *Yue et al.* [2002] was followed: the raw data were detrended by a

linear fit and the fitted series were prewhitened by removing the first order autoregressive component. A hypothesis test for trend (slope) was then conducted on the linear combination of the trend in the raw data and the residuals of the prewhitened data using the Mann-Kendall tau test on a fitted Kendall-Theil regression line [*Helsel and Hirsch*, 1992]. Trends in time series without significant autocorrelation were evaluated with linear regression and standard *t* tests were used to establish the significance of the slope parameter of the fitted regression line.

[30] Locally weighted scatterplot smoothing (LOWESS) curves [*Cleveland*, 1979; *Cleveland and Devlin*, 1988] were fit to variables lacking significant ($p < 0.01$) trends using the R statistical package (R Project for Statistical Computing, 2007, <http://www.r-project.org>). LOWESS curves objectively reflect the underlying characteristics of the data in the time series that may otherwise not be evident.

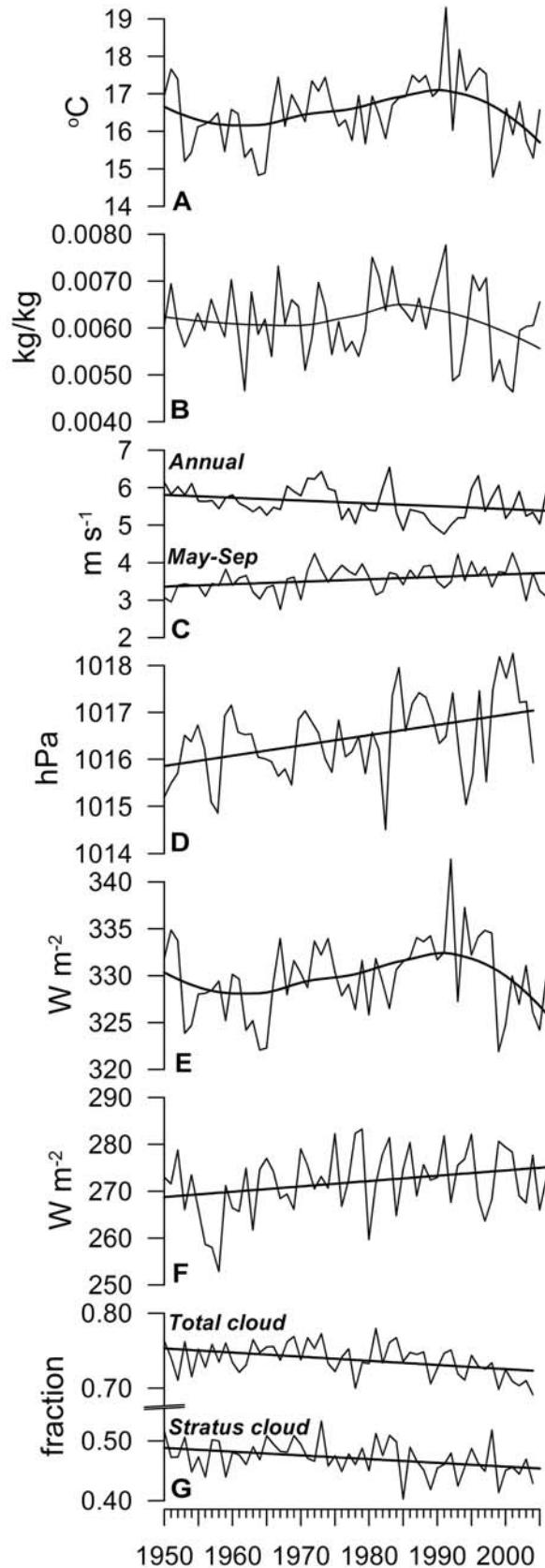
[31] The inflow of the Williamson and outflow of the Link River and A-Canal exhibit statistically significant trends and their time series are highly correlated ($r = -0.97$) over the 1950–2005 period (Figures 5b and 5d). From 1950 to 1980, the area of irrigated farmland in the Williamson and Sprague basins increased steadily, and has remained essentially constant since 1980 (Figure 5b). *Risley and Laenen* [1998] suggest that the combined increase in the use of surface and groundwater in the basins may be a contributing factor to the decrease in the discharge of the Williamson River into UKL. The effect of irrigation cannot be ruled out as an influence; however, little is known about the actual volume of basin-wide water withdrawals for irrigation and the dynamics of irrigation returns to the river and to groundwater recharge.

[32] The PRISM precipitation data do not have a significant trend; the LOWESS fit (Figure 5c) suggests a weak increasing tendency over the last 20 years of the record, but that tendency is leveraged by wet periods in the 1980s and again in the mid-1990s. The lack of association with the trend in Williamson River inflow indicates the dominance of higher elevation controls of the long-term water balance. Significant trend is present in the time series of simulated annual evaporation (Figure 5e). The more anomalous wet (dry) years and periods tend to be accompanied by low (high) evaporation through climatic coupling.

[33] Operational and climatic controls are both evident in the time series of lake surface area (Figures 5a and 5b). Control of the surface area through operation of the Link River Dam complicates and weakens any climatically determined trend that may have been present (the trend was significant at $p = 0.17$ level). The LOWESS fit to lake surface area suggests a transition toward generally reduced surface areas after the early 1980s. Modulation of simulated evaporation (Figure 5e) by changes in lake area (Figure 5a) eliminates the trend and produces a time series of volumetric water loss (Figure 5f) that differs substantially from a time series that would be generated by assuming a fixed evaporation rate. The mean and maximum of the difference between the volumetric time series is $-2.2 \times 10^7 \text{ m}^3$ (18,242 acre feet) and $-5.1 \times 10^7 \text{ m}^3$ (40,669 acre feet), respectively.

[34] The trends in the water balance components of UKL are the result of climatic trends over the lake and its catchment. Analysis of the May–September time series of

meteorological variables that determine evaporation indicates the controls of the positive trend in evaporation. Neither the 1950–2005 time series of air temperature (Figure 6a) nor the time series of specific humidity (Figure 6b)



have statistically significant trends (computed values of $p < 0.2$ and $p < 0.6$, respectively). The LOWESS fit to temperature suggests a tendency for warming through the mid-1990s with cooling thereafter. Specific humidity (Figure 6b) also displays a tendency for reduced atmospheric moisture beginning in the 1990s. The lack of a sustained warming trend at the lake differs from the trends in temperature at higher elevation sites in the basin (Figures 7a and 7b). On an annual basis, wind speed displays a small but statistically significant negative trend while May–September wind speed displays a slight positive trend (Figure 6c). The increase in May–September winds is associated with the trend in sea level pressure (Figure 6d).

[35] Radiative inputs to the lake also changed over the 1950–2005 period. The time series of longwave radiation, computed as a function of the blended air temperature data, displays similar properties in lacking a significant linear trend and displaying a ~ 30 year increasing tendency followed by a decreasing tendency at the end of the period (Figure 6e). A positive trend in May–September incident solar radiation over the period (Figure 6f) is associated with trends toward decreased total and stratus (nonconvective) cloud cover (Figure 6g).

[36] Pearson correlation analysis of annual evaporation and the variables affecting evaporation indicated significant correlations with solar radiation ($r = 0.5$, $p < 0.001$), air temperature ($r = 0.3$, $p < 0.05$), longwave radiation ($r = 0.3$, $p < 0.05$), specific humidity ($r = 0.5$, $p < 0.001$) over the 1950–2005 period. The positive trend in simulated evaporation is thus explained by similar trends in radiative inputs and a slight decrease in atmospheric water vapor content. Although no statistically significant relationship was found between evaporation and wind speed (wind speed does have a positive trend for the period (Figure 5c)), the apparent trend in wind speed also contributed to the trend in evaporation.

[37] Trends toward predominantly warmer and drier conditions are evident in the higher elevations of the UKL catchment. Both the simulated 2 m air temperature from the RegCM grid boxes representing the basin and air temperature measurements at Crater Lake display statistically significant warming trends (Figures 7a and 7b). Shorter records (1990–2005) from two SNOTEL sites in and just out of the UKL basin (Figure 7b) also have statistically significant warming trends; however, the limited length of the records overemphasizes the rate of change. Negative trends in annual precipitation are significant in the observed record for Crater Lake, the RegCM, and SNOTEL sites in the basin (Figures 7c and 7d). The reduction in precipitation is reflected in trends in both the snow water equivalent (SWE) and fractional snow cover simulated by the RegCM

Figure 6. Time series of 1950–2005 simulated and observed atmospheric variables related to evaporation. The plots are for the May–September peak evaporation season, unless indicated otherwise. Linear trend lines indicate statistically significant trends (at the $p < 0.1$ level and greater) and LOWESS fits indicate lack of significant linear trend. (a) air temperature from the RegCM2/NOAA blended data, (b) specific humidity, (c) wind speed, (d) sea level pressure, (e) atmospheric longwave radiation, (f) incident solar radiation, and (g) total cloud and stratus cloud cover (note break in the ordinate).

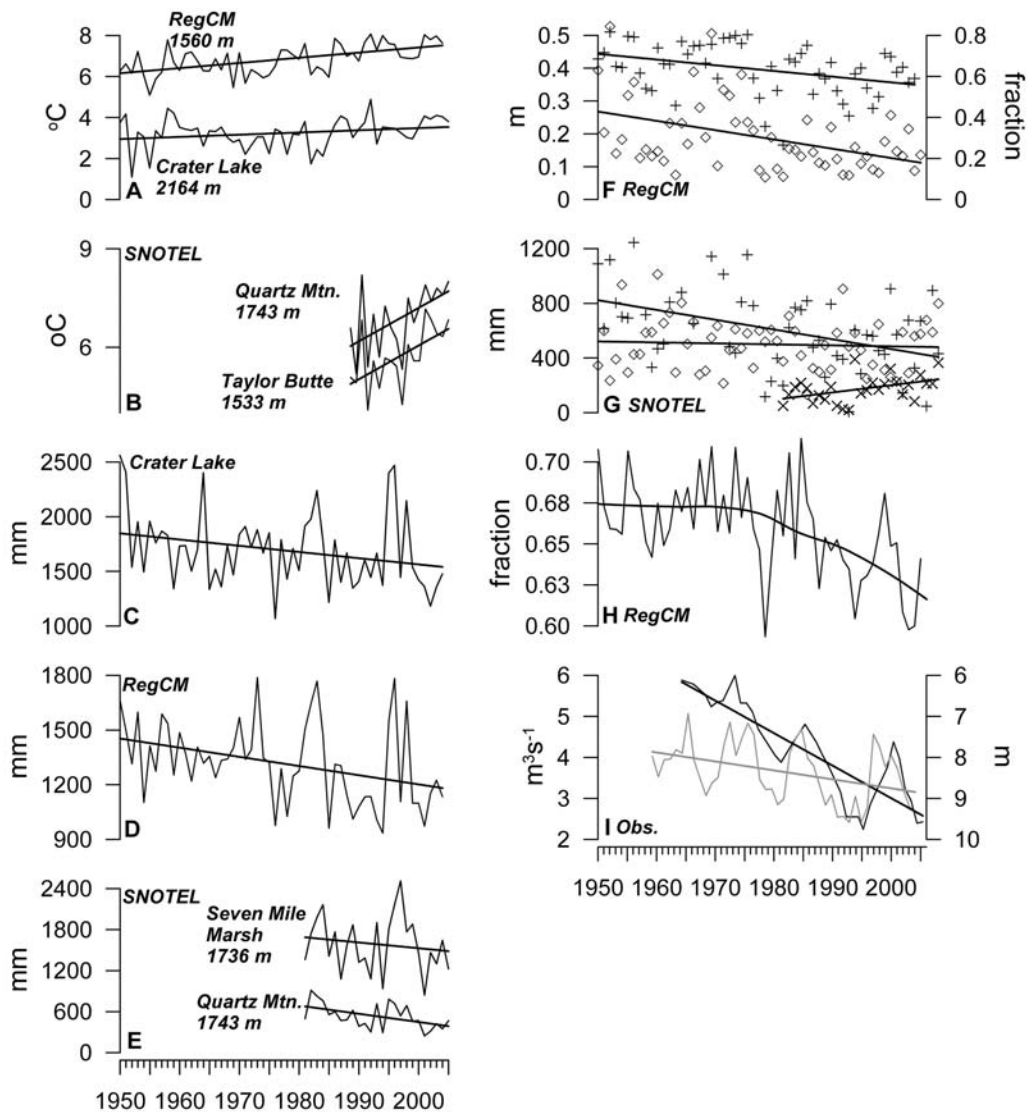


Figure 7. Annual time series of 1950–2005 simulated and observed variables for the UKL basin. Statistically significant trends (at the $p < 0.1$ level and greater) are indicated by linear fits and LOWESS curves are fit to time series lacking significant trend. (a) Annual air temperature simulated by RegCM and measured at Crater Lake; (b) annual air temperature for the Quartz Mountain and Taylor Butte NRCS SNOTEL sites with elevation in meters; (c) precipitation measured at Crater Lake; (d) precipitation simulated by RegCM; (e) annual precipitation at the Seven Mile Marsh and Quartz Mountain NRCS SNOTEL sites with elevation in meters; (f) snow water equivalent (SWE) (pluses) fit with a trend line (thin line), left ordinate and fractional snow cover (circles) fit with a trend line, right ordinate simulated by RegCM; (g) trends in SWE fit to the NRCS SNOTEL data for Billie Creek Divide (pluses), Summer Rim (circles), and Taylor Butte (circles), H: 5-cm soil moisture simulated by RegCM, and I: March 15 depth to water in USGS well 422508121161501 36S_12E-28ADA located ~ 50 km east of UKL (thick line, right ordinate) and annual discharge in Fall River, a groundwater source stream located ~ 150 km north of UKL (thin line, left ordinate).

(Figure 7f) and the Billie Creek Divide SNOTEL site (Figure 7g). The Summer Rim SNOTEL site has no trend, whereas the shorter record (1981–2005) for Taylor Butte has a statistically significant positive trend (Figure 7g). For the 1981–2005 period, the total SWE at Taylor Butte was $\sim 35\%$ of the total SWE at Billie Creek Divide indicating the dominant role the Cascade range plays in supplying runoff for both streamflow and groundwater recharge in the UKL basin [Gannett *et al.*, 2007].

[38] Significant trends are also found in the time series of simulated precipitation from the RegCM and in precipitation measurements at Crater Lake (Figures 7c and 7d). The nonlinearity and thus higher-order autoregressive nature of soil moisture (Figure 7h) precludes simple trend analysis, but the LOWESS fit clearly displays a drying tendency after the large reduction in 1977–1978. Although there has been an apparent trend toward decreasing snow water over the period, the LOWESS fits also suggest the possibility of a more stepwise transition during the mid- to late-1970s. The

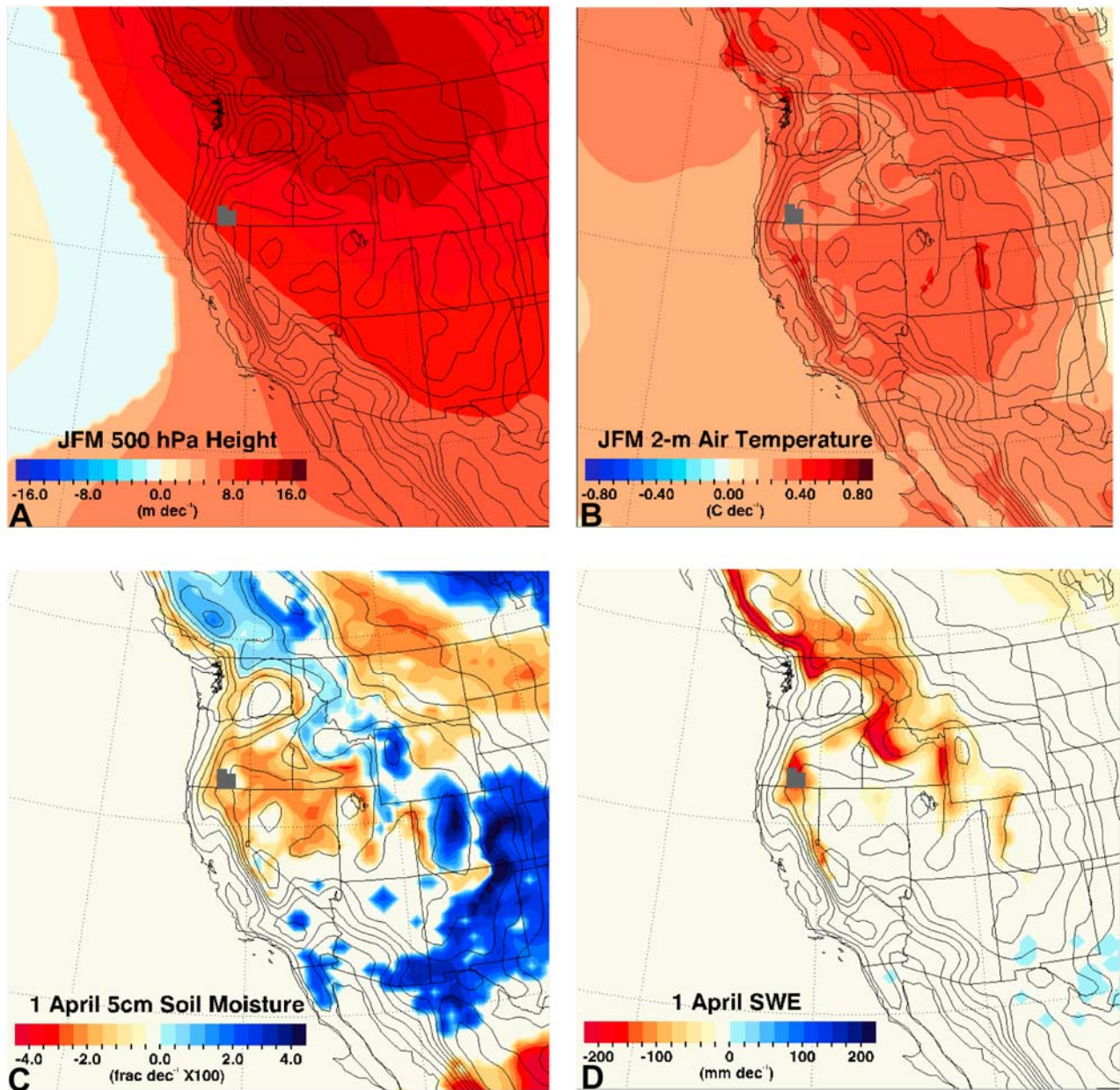


Figure 8. Decadal trends in simulated RegCM fields. The gray rectangle represents the location of the UKL basin. (a) January–March 500 hPa height, (b) January–March 2 m air temperature, (c) April 1 5 cm soil moisture, and (d) April 1 snow-water equivalent.

existence of this regime shift has been described as a property of the Pacific Decadal Oscillation (PDO) [McGowan *et al.*, 1998; Hare and Mantua, 2000], but it could also be attributed to low-frequency climate variability in North Pacific sea surface temperatures [Rudnick and Davis, 2003]. Evidence of a regionally synchronous drying trend in the UKL basin is also present and statistically significant in the time series of water level in a well located ~ 50 km east of UKL, and in a spring-fed river ~ 150 km north of UKL (Figure 7i), suggesting that the responses in the UKL basin are imbedded in regional scale climate changes.

[39] The trends in the water and atmospheric variables of the UKL basin are part of broader, regional-scale climate trends that occurred from 1950 to 2005 (Figure 8). During this period, wintertime 500 hPa heights increased

(Figure 8a) with an associated positive trend in surface air temperatures (Figure 8b), consistent with observed trends in the basin and trends in Northern Hemisphere temperatures [Mann and Jones, 2003; Intergovernmental Panel on Climate Change, 2007]. April 1 soil moisture levels over the northern Great Basin and the Pacific Northwest have trended to drier conditions (Figure 8c) as a result of warming and reductions in winter moisture and snowpack (Figures 8a, 7c, and 7d) [Mote, 2003, 2006].

[40] Additional insight into the climate-driven hydrologic trends is provided by considering decadal changes within the context of longer time series (Figure 9). Inflow and outflow to the lake were relatively low from 1920 through the late 1940s when sustained increases in precipitation resulted in corresponding increases in water to the lake.

Water supply peaked in the 1950s and trended to drier conditions thereafter (Figures 9b–9d). The drying trend is coincident with the warming and related drying trend over the basin discussed previously (Figure 7) which, in turn,

are consistent with observed Northern Hemisphere warming over the past century (Figures 9a and 9b). Variability in the water inputs and outputs is modulated by some of the stronger SOI, PDO, and NAO events [e.g., McCabe and Dettinger, 2002], but the overall trend to less water availability in the basin is most likely attributable to hemispheric warming.

7. Discussion

[41] Climatically controlled evaporation from UKL can be simulated with reasonable accuracy using input derived from meteorological observations from the lake, from weather stations distant from the lake, and from output from a regional climate model. Although the long-term average evaporation rate is similar to that calculated from pan values (using a pan coefficient of 0.7), the climatically determined nonstationary trend in simulated lake evaporation contrasts with a fixed evaporation rate based on pan estimates. Interannual and longer multiyear variability is not reflected by a fixed, pan-based value and is thus better captured by the lake model, suggesting the desirability of using the model to calculate near-real-time values during peak evaporation season to reduce uncertainties in the estimates of the UKL water balance.

[42] The primary components of the UKL water balance exhibit statistically significant trends over the 1950–2005 period. These trends can be attributed to climate and water-related variables that have changed at higher elevations of the basin, and to trends in atmospheric circulation and surface water and energy balance components. The trend in the time series of Williamson River flows is associated significantly with the trends in Crater Lake precipitation and air temperature and snow water equivalent simulated by the RegCM. Decadal trends identified in climate in the observed data and in the data simulated by the RegCM are consistent with a number of studies [Dettinger and Cayan, 1995; Hodge et al., 1998; Mote, 2003, 2006; Howat and Tulaczyk, 2005a, 2005b; Pepin et al., 2005; Howat et al., 2006; Barnett et al., 2008].

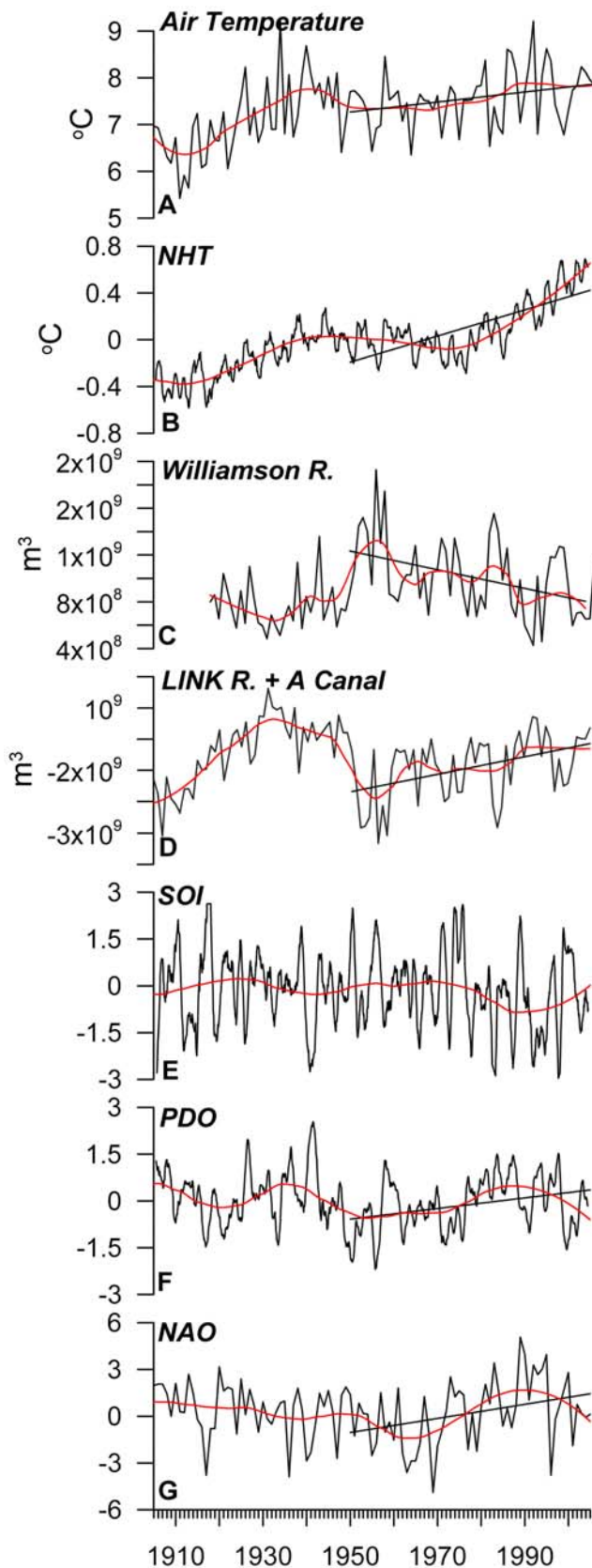


Figure 9. Long-term time series of raw data (black), LOWESS fits (red) and 1950–2004 trend lines (black). Trend lines are significant at the $p < 0.1$ level and greater; SOI exhibits no significant trend. (a) PRISM air temperature over the UKL basin, (b) annual Northern Hemisphere temperature anomalies (NHT), (c) Williamson River inflow, (d) total outflow and change in lake storage (Link River plus A-Canal), (e) the Southern Oscillation Index (SOI), (f) the Pacific Decadal Oscillation (PDO), and (g) the North Atlantic Oscillation (NAO). SOI data are from the Climate Analysis Section at the National Center for Atmospheric Research (<http://www.cgd.ucar.edu/cas/catalog/climind/soi.html>) [Trenberth, 1984], PDO data are from the Joint Institute for Study of the Atmosphere and Ocean, University of Washington (<http://jisao.washington.edu/pdo/>), NAO data are from the Climate Analysis Section at the National Center for Atmospheric Research (<http://www.cgd.ucar.edu/cas/jhurrell/indices.html#refinfo>) [Hurrell, 1995] and NH temperature data from the Climate Research Unit of the University of East Anglia, UK (<http://www.cru.uea.ac.uk/cru/>).

[43] Over the annual and longer time scales considered here, climatic controls dominate the water balance of the lake; strong evidence of the effects of water management in the UKL is not apparent. Important management decisions affecting the basin, for example, those regarding irrigation water allocations and meeting requirements of the endangered species in UKL, are made on a year-by-year basis within the context of climate-driven interannual variability in water supply. The 1950–2005 period analyzed here is imbedded in longer term climate variability in the UKL basin. The association of the trends within the longer historical records suggests that drying over the last six decades may well continue to persist and present additional challenges to water managers in the basin.

[44] **Acknowledgments.** This manuscript reflects thoughtful and thorough reviews by M. Gannet, J. Risley, T. Wood, D. Zahnle and three anonymous journal reviewers. I thank P. Bartlein for numerous discussions and critiques of the research. The quality and integrity of the data collected at UKL were ensured by G. Hoilman, M. Johnston and M. Lindenberg of the USGS.

References

- Allen, R. G., et al. (2005), The ASCE standardized reference evaporation equation, 56 pp., Am. Soc. of Civ. Eng., Reston, Va.
- Anderson, E. R. (1954), Energy-budget studies, in *Water-Loss Investigations: Lake Hefner Studies, U.S. Geol. Surv. Prof. Pap.*, 269, 71–119.
- Barnett, T. P., et al. (2008), Human-induced changes in the hydrology of the western United States, *Science*, 319, 1080–1083, doi:10.1126/science.1152538.
- Bidlake, W. R. (2002), Evapotranspiration from selected fallowed agricultural fields on the Tule Lake National Wildlife Refuge, California, during May to October 2000, *U.S. Geol. Surv. Water Resour. Invest. Rep.*, 02-4055, 71 pp.
- Box, G. E. P., and G. M. Jenkins (1976), *Time Series Analysis, Forecasting, and Control*, 575 pp., Holden-Day, San Francisco, Calif.
- Bradbury, J. P., S. M. Colman, and R. L. Reynolds (2004), The history of recent limnological changes and human impact on Upper Klamath Lake, Oregon, *J. Paleolimnol.*, 31, 151–165, doi:10.1023/B:JOPL.0000019233.12287.18.
- Braunworth, W. S., Jr., T. Welch, and R. Hathaway (Eds.) (2001), Water allocation in the Klamath Reclamation Project: An assessment of natural resource, economic, social and institutional issues with a focus on the Upper Klamath Basin, *Spec. Rep. 1037*, 401 pp., Ext. Serv., Oreg. State Univ., Corvallis.
- Brutsaert, W. F. (1982), *Evaporation Into the Atmosphere*, 299 pp., D. Reidel, Dordrecht, Netherlands.
- Cleveland, W. S. (1979), Robust locally weighted regression and smoothing scatterplots, *J. Am. Stat. Assoc.*, 74, 829–836, doi:10.2307/2286407.
- Cleveland, W. S., and S. J. Devlin (1988), Locally weighted regression: An approach to regression analysis by local fitting, *J. Am. Stat. Assoc.*, 83, 596–610, doi:10.2307/2289282.
- Daly, C., R. P. Neilson, and D. L. Phillips (1994), A statistical-topographic model for mapping climatological precipitation over mountainous terrain, *J. Appl. Meteorol.*, 33, 140–158, doi:10.1175/1520-0450(1994)033<0140:ASTMFM>2.0.CO;2.
- Dettinger, M. D., and D. R. Cayan (1995), Large-scale atmospheric forcing of recent trends toward early snowmelt runoff in California, *J. Clim.*, 8, 606–623, doi:10.1175/1520-0442(1995)008<0606:LSAFOR>2.0.CO;2.
- Drexler, J. Z., R. L. Snyder, D. Spano, K. Tha, and U. Paw (2004), A review of models and micrometeorological methods used to estimate wetland evapotranspiration, *Hydrol. Processes*, 18, 2071–2101, doi:10.1002/hyp.1462.
- Dutton, J. A., and R. A. Bryson (1962), Heat flux in Lake Mendota, *Limnol. Oceanogr.*, 7(1), 88–97.
- Gannett, M. W., K. E. Lite Jr., D. S. Morgan, and C. A. Collins (2001), Ground-water hydrology of the upper Deschutes Basin, Oregon, *U.S. Geol. Surv. Water Resour. Invest. Rep.*, 00-4162, 78 pp.
- Gannett, M. W., K. E. Lite Jr., J. L. La Marche, B. J. Fisher, and D. J. Polette (2007), *Ground-water hydrology of the Upper Klamath Basin, U.S. Geol. Surv. Sci. Invest. Rep.*, 2007-5050, 84 pp.
- Giorgi, F., M. R. Marinucci, and G. T. Bates (1993), Development of a second-generation regional climate model (RegCM2). Part I: Boundary-layer and radiative transfer processes, *Mon. Weather Rev.*, 121, 2794–2813, doi:10.1175/1520-0493(1993)121<2794:DOASGR>2.0.CO;2.
- Hare, S. R., and N. J. Mantua (2000), Empirical evidence for North Pacific regime shifts in 1977 and 1989, *Prog. Oceanogr.*, 47(2–4), 103–146.
- Helsel, D. R., and R. M. Hirsch (1992), *Statistical Methods in Water Resources, Stud. Environ. Sci.*, vol. 49, 522 pp., Elsevier, New York.
- Henderson-Sellers, B. (1985), New formulation of eddy diffusion thermocline models, *Appl. Math. Modell.*, 9, 441–446, doi:10.1016/0307-904X(85)90110-6.
- Henderson-Sellers, B. (1986), Calculating the surface energy balance for lake and reservoir modeling: A review, *Rev. Geophys.*, 24(3), 625–649, doi:10.1029/RG024i003p00625.
- Hodge, S. M., D. C. Trabant, R. M. Krimmel, T. A. Heinrichs, R. S. March, and E. G. Josberger (1998), Climate variations and changes in mass of three glaciers in western North America, *J. Clim.*, 11, 2161–2179, doi:10.1175/1520-0442(1998)011<2161:CVACIM>2.0.CO;2.
- Hostetler, S. W., and P. J. Bartlein (1990), Modeling climatically determined lake evaporation with application to simulating lake-level variations of Harney-Malheur Lake, Oregon, *Water Resour. Res.*, 26(10), 2603–2612.
- Hostetler, S. W., and F. Giorgi (1993), Use of high-resolution climate model data in landscape-scale hydrologic models: A demonstration, *Water Resour. Res.*, 29(6), 1685–1695, doi:10.1029/93WR00263.
- Hostetler, S. W., and F. Giorgi (1995), Effects of 2 × CO₂ climate on two large lake systems: Pyramid Lake, Nevada, and Yellowstone Lake, Wyoming, *Global Planet. Change*, 10, 43–54, doi:10.1016/0921-8181(94)00019-A.
- Hostetler, S. W., and E. E. Small (1999), Response of North American lakes to simulated climate change, *J. Am. Water Resour. Assoc.*, 35(6), 1625–1637, doi:10.1111/j.1752-1688.1999.tb04241.x.
- Hostetler, S. W., P. J. Bartlein, and J. O. Holman (2006), Atlas of climatic controls of wildfire in the western United States, *U.S. Geol. Surv. Sci. Invest. Rep.*, 2006-5139. (Available at <http://pubs.usgs.gov/sir/2006/5139>)
- Howat, I. M., and S. Tulaczyk (2005a), Climate sensitivity of spring snowpack in the Sierra Nevada, *J. Geophys. Res.*, 110, F04021, doi:10.1029/2005JF000356.
- Howat, I. M., and S. Tulaczyk (2005b), Trends in California's snow water volume over a half century of climate warming, *Ann. Glaciol.*, 40, 151–156, doi:10.3189/17275640578183816.
- Howat, I. M., S. Tulaczyk, P. Rhodes, K. Isreal, and M. Snyder (2006), A precipitation-dominated, mid-latitude glacier system: Mount Shasta, California, *Clim. Dyn.*, 28, 85–98, doi:10.1007/s00382-006-0178-9.
- Hubbard, L. L. (1970), Water budget of Upper Klamath Lake, southwestern Oregon, in *U.S. Geol. Surv. Hydrol. Invest. Atlas, HA-351*, scale 1:250,000.
- Hurrell, J. W. (1995), Decadal trends in the North Atlantic Oscillation: Regional temperatures and precipitation, *Science*, 269, 676–679, doi:10.1126/science.269.5224.676.
- Intergovernmental Panel on Climate Change (2007), *Climate Change 2007: The Physical Science Basis. Contribution of Working Group I to the Fourth Assessment Report of the Intergovernmental Panel on Climate Change*, edited by S. Solomon et al., Cambridge Univ. Press, Cambridge, U. K.
- Kahler, D. M., and W. Brutsaert (2006), Complementary relationship between daily evaporation in the environment and pan evaporation, *Water Resour. Res.*, 42, W05413, doi:10.1029/2005WR004541.
- Kistler, R., et al. (2001), The NCEP-NCAR 50-year reanalysis: Monthly means CDROM and documentation, *Bull. Am. Meteorol. Soc.*, 82, 247–267, doi:10.1175/1520-0477(2001)082<0247:TNNYRM>2.3.CO;2.
- Mann, M. E., and P. D. Jones (2003), Global surface temperature over the past two millennia, *Geophys. Res. Lett.*, 30(15), 1820, doi:10.1029/2003GL017814.
- Masoner, J. R., D. I. Stannard, and S. C. Christenson (2008), Differences in evaporation between a floating pan and class A pan on land, *Water Resour. Bull.*, 44(3), 552–561, doi:10.1111/j.1752-1688.2008.00181.x.
- McCabe, G. J., and M. D. Dettinger (2002), Primary modes and predictability of year-to-year snowpack variations in the western United States from teleconnections with the Pacific Ocean climate, *J. Hydrometeorol.*, 3, 13–25, doi:10.1175/1525-7541(2002)003<0013:PMAPOY>2.0.CO;2.
- McGowan, J. A., D. R. Cayan, and L. M. Dorman (1998), Climate-ocean variability and ecosystem response in the northeast Pacific, *Science*, 281, 210–217, doi:10.1126/science.281.5374.210.
- Miller, W. E., and J. C. Tash (1967), Upper Klamath Lake studies, Oregon, *Water Pollut. Control Ser. ap. WP-20-8*, 37 pp., Pac. Northwest Lab., Fed. Water Pollut. Control Admin., Corvallis, Oreg.

- Morace, J. L. (2007), Relation between selected water-quality variables, climatic factors, and lake levels in Upper Klamath and Agency Lakes, Oregon, 1990–2006, *U.S. Geol. Surv. Sci. Invest. Rep.*, 2007-5117, 54 pp.
- Mote, P. W. (2003), Trends in snow water equivalent in the Pacific Northwest and their climatic causes, *Geophys. Res. Lett.*, 30(12), 1601, doi:10.1029/2003GL017258.
- Mote, P. W. (2006), Climate-driven variability and trends in mountain snowpack in western North America, *J. Clim.*, 19, 6209–6220, doi:10.1175/JCLI3971.1.
- National Research Council (2008), *Hydrology, Ecology, and Fishes of the Klamath River Basin*, 250 pp., Natl. Acad., Washington, D. C.
- Pepin, N. C., M. Losleben, M. Hartman, and K. Chowanski (2005), A comparison of SNOTEL and GHCN/CRU surface temperatures with free-air temperatures at high elevations of the western United States: Data compatibility and trends, *J. Clim.*, 18, 1967–1985, doi:10.1175/JCLI3375.1.
- Perry, T., T. Mull, A. Leib, A. Harrison, E. Cohen, R. Rasmussen, and J. Hicks (2004), Undepleted natural flow of the Upper Klamath River, final draft report, 148 pp., Tech. Serv., U.S. Bur. of Reclam., Denver, Colo. (Available at <http://klamathwaterlib.oit.edu/>)
- Risley, J. C., and M. W. Gannett (2006), An evaluation and review of water-use estimates and flow data for the Lower Klamath and Tule Lake National Wildlife Refuges, Oregon and California, *U.S. Geol. Surv. Sci. Invest. Rep.*, 2006-5036, 18 pp.
- Risley, J. C., and A. Laenen (1998), Upper Klamath Lake Basin nutrient-loading study—Assessment of historic flows in the Williamson and Sprague rivers, *U.S. Geol. Surv. Sci. Invest. Rep.*, 98-4198, 28 pp.
- Rudnick, D. L., and R. E. Davis (2003), Red noise and regime shifts, *Deep Sea Res., Part I*, 50, 691–699, doi:10.1016/S0967-0637(03)00053-0.
- Small, E. E., L. C. Sloan, S. W. Hostetler, and F. Giorgi (1999), Simulating the water balance of the Aral Sea with a coupled climate-lake model, *J. Geophys. Res.*, 104(D6), 6583–6602, doi:10.1029/98JD02348.
- Snyder, D. T., and J. L. Morace (1997), Nitrogen and phosphorus loading from drained wetlands adjacent to Upper Klamath and Agency lakes, Oregon, *U.S. Geol. Surv. Sci. Invest. Rep.*, 97-4059, 73 pp.
- Snyder, R. L., M. Orang, S. Matyac, and M. E. Grismer (2005), Simplified estimation of reference evapotranspiration from pan evaporation data in California, *Irrig. Drain. Eng.*, 131(3), 249–253, doi:10.1061/(ASCE)0733-9437(2005)131:3(249).
- Thompson, S. L., and D. Pollard (1995), A global climate model (GENESIS) with a land-surface transfer scheme (LSX). Part I: Present climate simulation, *J. Clim.*, 8, 732–761, doi:10.1175/1520-0442(1995)008<0732:AGCMWA>2.0.CO;2.
- Trenberth, K. E. (1984), Signal versus noise in the Southern Oscillation, *Mon. Weather Rev.*, 112, 326–332, doi:10.1175/1520-0493(1984)112<0326:SVNITS>2.0.CO;2.
- von Storch, H., and F. W. Zwiers (1999), *Statistical Analysis in Climate Research*, 484 pp., Cambridge Univ. Press, Cambridge, U. K.
- Wood, T. M., G. R. Hoilman, and M. K. Lindenberg (2006), Water-quality conditions in Upper Klamath Lake, Oregon, 2002–04, *U.S. Geol. Surv. Sci. Invest. Rep.*, 2006-5209, 52 pp.
- Wood, T. M., R. T. Cheng, J. W. Gartner, G. R. Hoilman, M. K. Lindenberg, and R. E. Wellman (2008), Modeling hydrodynamics and heat transport in Upper Klamath Lake, Oregon, and implications for water quality, *U.S. Geol. Surv. Sci. Invest. Rep.*, 2008-5076, 48 pp. (Available at <http://pubs.usgs.gov/sir/2008/5076/>)
- Yue, S., P. Pilon, B. Phinney, and G. Cavadias (2002), The influence of autocorrelation on the ability to detect trends in hydrological series, *Hydrol. Processes*, 16, 1807–1829, doi:10.1002/hyp.1095.

S. W. Hostetler, U.S. Geological Survey, Department of Geosciences, Oregon State University, Corvallis, OR 97331, USA. (steve@coas.oregonstate.edu)